INTERNATIONAL JOURNAL OF CLIMATOLOGY
*Int. J. Climatol.* **33**: 1280–1292 (2013)
Published online 17 May 2012 in Wiley Online Library
(wileyonlinelibrary.com) DOI: 10.1002/joc.3513

RMetS
Royal Meteorological Society

# The 'spring predictability barrier' for ENSO predictions and its possible mechanism: results from a fully coupled model

Wansuo Duan[a]* and Chao Wei[b]

[a] *LASG, Institute of Atmospheric Physics, Chinese Academy of Sciences, Beijing, China*
[b] *National Climate Center, Chinese Meteorology Administration, Beijing, China*

**ABSTRACT:** Using predictions for the sea surface temperature (SST) generated by a Flexible Global Ocean-Atmosphere-Land System model of IAP/LASG (FGOALS-g), the season-dependent predictability of SST anomalies for El Nino/La Nina events is investigated by analyzing the forecast error growth in an imperfect model scenario. The results indicate that, for the predictions through the spring season in the growth phase of El Nino events, the prediction errors induced by both initial errors and model errors tend to have a prominent season-dependent evolution and yield a prominent spring predictability barrier (SPB). For the decay-phase predictions of El Nino events, a less prominent season-dependent evolution of prediction errors and then a less prominent SPB are observed. For the growth- and decay-phase predictions of La Nina events, the prediction errors do not exhibit a significant season-dependent evolution and yield a less prominent SPB phenomenon. These results indicate that the SPB phenomenon depends remarkably on the ENSO events themselves, particularly the phases of the El Nino/La Nina events. We also report that the initial SST errors that correspond to a significant SPB for El Nino events tend to have the dominant modes in a large-scale dipolar pattern with negative anomalies in the equatorial central-western Pacific and positive anomalies in the eastern Pacific, or vice versa. We further demonstrate that the error growth related to a significant SPB for El Nino prediction generated by the FGOALS-g model can result from two dynamical mechanisms: in one case, the prediction errors grow in a manner similar to El Niño; in the other, the prediction errors develop with a tendency opposite to El Niño. Copyright © 2012 Royal Meteorological Society

KEY WORDS ENSO; predictability; error growth

*Received 7 March 2011; Revised 28 March 2012; Accepted 15 April 2012*

## 1. Introduction

The El Niño-Southern Oscillation (ENSO) cycle, a fluctuation between unusually warm (El Niño) and cold (La Niña) conditions, is the most prominent year-to-year climate variation on earth. Although ENSO originates and develops mainly in the tropical Pacific through interactions between the ocean and the atmosphere, its environmental and socioeconomic impacts are felt worldwide. Knowledge about the ENSO cycle and the ability to forecast its variations, however limited at present, supply valuable information for agriculture, public health and safety, fisheries, forestry, and many other spheres of climate-sensitive human endeavors.

Numerous models have been developed to simulate and predict ENSO events. These models range from theoretical simulations (Wang and Fang, 1996; Jin, 1997a, 1997b; Wang *et al*., 1999) through so-called intermediate coupled models (Zebiak and Cane, 1987; McCreary and Anderson, 1991; Kleeman *et al*., 1995) to complex coupled general circulation models (CGCMs). Both intermediate coupled models (Zebiak and Cane, 1987; Kleeman, 1993) and CGCMs have been used to forecast the ENSO cycle. Recently, the climate forecast system at the National Center for Environmental Prediction (NCEP) (Saha *et al*., 2006), the seasonal forecast systems at the European Center for Medium-Range Weather Forecasts (ECMWF), and the Multi-model Ensemble System (MME) at the EU (Palmer *et al*., 2004) and at the Asian-Pacific Economic Cooperation (APEC) Climate Center (APCC) have also been developed for seasonal to interannual climate predictions.

A detailed comparison of ENSO models was given by Kirtman *et al*. (2002), who indicated that it is difficult to tell which of these models demonstrates greater forecasting capabilities between the dynamical models and statistical models or between the intermediate models and complex models. Furthermore, these models reveal a consistent characteristic of ENSO predictions: if forecasts are made before and through the spring, the ENSO predictions tend to be much less successful. This low predictability is the so-called "spring predictability barrier" (SPB) phenomenon of ENSO forecasts (Webster and Yang, 1992; Lau and Yang, 1996; Kirtman *et al*., 2002; McPhaden, 2003).

* Correspondence to: W. Duan, Institute of Atmospheric Physics, Chinese Academy of Sciences, Beijing 100029, China.
E-mail: duanws@lasg.iap.ac.cn

The SPB is a well-known characteristic of ENSO forecasts. The SPB does not only exist in coupled models but also in some statistical models (Kirtman *et al*., 2002). On some occasions, the SPB is even stronger in statistical models than in GCMs (van Oldenborgh *et al*., 2005). While significant progress has been made in ENSO theories and predictions over the years, especially through the TOGA (Tropical Ocean Global Atmosphere) program (see the review by Wang and Picaut 2004), considerable SPB phenomena still occur in realistic ENSO predictions (Jin *et al*., 2008; Luo *et al*., 2008). One therefore questions whether the SPB is an intrinsic characteristic of ENSO forecasts. Webster and Yang (1992) demonstrated that a possible cause of the SPB is the rapid seasonal transition of monsoon circulation during the boreal spring that perturbs the Pacific basic state when the east-west sea surface temperature (SST) gradient is the weakest. Another explanation proposed by Webster (1995) is that the SPB is due to the weak ocean–atmosphere coupling that occurs during the spring in the eastern Pacific. Other studies have argued that SST anomalies in the boreal spring are relatively small, such that these anomalies are difficult to detect and forecast in the presence of atmospheric and oceanic noises (Xue *et al*., 1994; Chen *et al*., 1995). These theories suggest that the causes of the SPB are related to intrinsic physical properties of ENSO, indicating that the SPB may be inherent in ENSO forecasts. Samelson and Tziperman (2001) also reported that SPB is an intrinsic characteristic of ENSO forecasting.

Other studies have indicated that the SPB can be reduced through appropriate approaches, which goes against the internality of the SPB demonstrated in some studies, including by Samelson and Tziperman (2001). Chen *et al*. (1995, 2004) suggested that the predictability barrier could be eliminated through improved initialization. McPhaden (2003) demonstrated that subsurface information has a winter persistence barrier and that the predictability of ENSO bestriding spring can be greatly enhanced by incorporating this information into the model. Recently, Mu *et al*. (2007a, 2007b) demonstrated that a 'significant SPB' might be a result of the combined effect of three factors: the climatological annual cycle, the El Nino event itself and the initial error pattern. The former two factors are robustly in existence for ENSO events, while the third factor is factitious and induced by the limitation of observational instruments, inaccurate initialization of the forecast models, etc. These results suggest that even if the seasonality of the annual cycle determined by observation, which is the origin of the seasonal dependence of error growth, is robust in forecast models, particular initial error modes are necessary to bring about the SPB (Mu *et al*., 2007a). That is to say, there exists the possibility that some types of initial errors may cause extreme uncertainties in ENSO forecasting through the spring and exhibit a prominent season-dependent evolution related to the SPB, due to the seasonality of ocean–atmosphere coupling. Other types of initial errors, however, tend to not yield a season-dependent evolution of error growth even though the annual cycle is embedded in the forecast models (Duan *et al*., 2009; Yu *et al*., 2009).

The 'significant SPB' mentioned here is the phenomenon that ENSO forecasting has a large prediction error; in particular, a prominent error growth occurs during the spring when the prediction is made before and throughout the spring (Mu *et al*., 2007a, 2007b). Nevertheless, it should be noted that the predictions that have a large prediction error but do not exhibit season-dependent evolution result in a less significant SPB; those with a trivial prediction error but a prominent seasonality of error growth also yield a less prominent SPB because the significant growth of error in the spring does not cause unacceptable prediction uncertainties. This clarification illustrates why we emphasize that a significant SPB entails not only a large prediction error but also a prominent seasonality of error growth. With this description of the 'significant SPB', Duan *et al*. (2009) and Yu *et al*. (2009) used the Zebiak–Cane model (Zebiak and Cane, 1987) to study the spatial characteristics of initial errors that cause 'a significant SPB' for ENSO events by performing perfect model predictability experiments with the approach of conditional nonlinear optimal perturbation (CNOP; Mu *et al*., 2003; Duan *et al*., 2004, 2008; Mu and Zhang, 2006; Duan and Mu, 2006). CNOP represents the initial error that induces the largest prediction error at the prediction time and has the potential for yielding a significant SPB (Mu *et al*., 2007a, 2007b; Yu *et al*., 2009). Using the CNOP method, Duan *et al*. (2009) and Yu *et al*. (2009) identified two types of CNOP-type initial errors that cause a significant SPB for El Nino events. One type possesses an SSTA component that has a large-scale zonal dipolar pattern with positive anomalies in the central equatorial Pacific and negative anomalies in the eastern equatorial Pacific; it tends to cause El Nino events to be under-predicted through spring. The other type has a pattern almost opposite to the former.

The experiments of Duan *et al*. (2009) and Yu *et al*. (2009) are perfect model predictability experiments, although the CNOP method tackles the evolution of finite-amplitude initial perturbation and has led to instructive results. In realistic predictions, there are typically both initial errors and model errors. Furthermore, the CNOPs are generally not computed in realistic predictions. We therefore naturally ask: do initial errors of realistic predictions exist that are similar to the CNOP errors and correspond to a significant SPB for El Nino events? What is the mechanism of the SPB for El Nino events in the imperfect model scenario?

In this paper, we will use the predictions generated by the Flexible Global Ocean Atmosphere Land System-gmail (FGOALS-g) model (see next section) for the sea surface temperature (SST; Yan and Yu, 2012), from the view of error growth, to investigate the characteristics of initial errors that correspond to a significant SPB in realistic ENSO predictions and to analyse the mechanism of the SPB in the imperfect model scenario. The paper is

 

organized as follows: in the next section, the predictions and the observations for SST are briefly introduced. In Section 3, the uncertainties of the ENSO forecasting generated by the FGOALS-g model and their season-dependent evolutions are presented. The characteristics of initial errors that correspond to a significant SPB are investigated in Section 4, which helps to determine whether the CNOP-like errors demonstrated by Duan *et al*. (2009) and Yu *et al*. (2009) exist in realistic ENSO predictions generated by the FGOALS-g model. On this basis, the effect of model errors on the SPB is discussed; the implications of these results are presented in Section 4. Finally, we summarize the results obtained in this paper and discuss them in Section 5.

## 2. The predicted and observed SST

The predictions used here are only for the monthly SST, which were generated by the FGOALS-g model (version 1.11) (Yan and Yu, 2012). The FGOALS-g model was a flexible coupled general circulation model (GCM) (Yu *et al*., 2002, 2004) developed by the State Key Laboratory of Numerical Modeling for Atmospheric Sciences and Geophysical Fluid Dynamics (LASG), Institute of Atmospheric Physics (IAP), Chinese Academy of Sciences. This model couples atmospheric, oceanic, land, and sea ice component models with the National Center for Atmospheric Research (NCAR) flux coupler.

The oceanic component is described by a LASG/IAP Climate System Ocean Model (LICOM) (Liu *et al*., 2004). This model involves 30 oceanic vertical layers with 12 equal levels in the upper 300 m; it treats the North Pole as an isolated island. The horizontal resolution of LICOM is $1^\circ \times 1^\circ$, and the domain covers from 75 °S to 88°N. The atmospheric component is a Grid-point Atmospheric Model of IAP/LASG (GAMIL), which includes a new dynamic core (Wang *et al*., 2004) and the physical parameterizations of the Community Atmospheric Model Version 2 (CAM2) of NCAR (Kiehl *et al*., 1996), except for a modified Tiedtke convective scheme (Li *et al*., 2007). The model employs a hybrid horizontal grid with a Gaussian grid of 2.8° between 65.58° N and 65.58° S and a weighted even-area grid elsewhere (Wang *et al*., 2004). Vertically, there are 26 $\sigma$-layers from the earth surface to 2.194 hPa.

The LICOM and GAMIL are coupled through a NCAR coupler (Kauffman and Large, 2002). A dynamical sea ice model known as the Community Sea Ice Model, version 4 (CSIM4) (Weatherly *et al*., 1998) and a land model known as the Community Land Model, version 2 (CLM2) (Bonan *et al*., 2002), are also coupled together. The frequency of coupling is 1 d for the oceanic model and 1 h for the atmospheric, land, and sea ice models.

Yan and Yu (2012) used this fully coupled model to predict the ENSO events during 1982–2005 and reported that the FGOALS-g model generated an acceptable forecast for ENSO events. The predictions capture the primary ENSO events during this period, and the anomaly correlation often exceeds 0.5 with a lead-time of 12 months. The predictions for SST are an ensemble forecast of ten different initial conditions of the atmospheric and land components with the same oceanic and sea ice initial conditions (Yan and Yu, 2012). By an SST nudging experiment, initial values of atmospheric and land components on January 1st, April 1st, July 1st, and October 1st from 1982 to 2005 were obtained. On these initial values, stochastic perturbations were superimposed and yielded ten initial conditions of an ensemble forecast. Each prediction was for a leading time of 12 months.

With the ten initial atmospheric and land conditions and the same initial oceanic and sea ice conditions, the FGOALS-g model generated ten single forecasts with a monthly SST related to ENSO predictions. For the month that the ENSO prediction begins, we use the mean of the SST during this month as the initial SST to study the behaviour of the prediction errors in this study. For example, for the initial time of April 1st, the mean SST in April was regarded as the initial SST. As such, for a start month, ten different atmospheric initial conditions correspond to ten different initial monthly SSTs. Therefore, we regarded January, April, July and October as the start months of the predictions. The mean of the ten single forecasts with ten initial monthly SSTs yields the result of the ensemble forecast. In this study, we adopted not only the products of the single forecasts but also those of the ensemble forecasts.

The predictions were compared to the 'observed' monthly SST in the Nino 3.4 area. For the period of 1982–2005, the so-called optimum interpolation monthly SST is used (Reynolds *et al*., 2002). These data were evaluated from the observed SST, satellite remote sensing, and numerical modelling data by the optimal interpolating method, which covered the period from November 1981 through March 2010 and the regions (89.5 °S–89.5 °N, 0.5 °E–0.5 °W) with a resolution of $1^\circ \times 1^\circ$. The predicted SST had the same resolution as the observation.

From 1982 to 2005, five typical El Nino events 1982/1983, 1986/1987, 1991/1992, 1997/1998 and 2002/2003 and four La Nina events 1984/1985, 1988/1989, 1995/1996 and 1998/1999 occurred. In this paper, we investigated the season-dependent predictability of the SST anomalies (SSTA) of the ENSO events. Because the predictions for the 1982/1983 El Nino event did not consist of the whole episode of the observed event, we only considered the other four El Nino events and the four La Nina events (Figure 1).

In this paper, we use Year (0) to denote the year when El Nino/La Nina attained a peak value and Year (−1) and Year (1) to signify the years before and after Year (0), respectively. The El Nino/La Nina predictions made with a start month of July (−1) (i.e., July in Year (−1)), October (−1), January (0) (i.e., January in Year (0)), and April (0) pass through the spring in the growth phase of El Nino/La Nina. For convenience, we hereafter refer

 

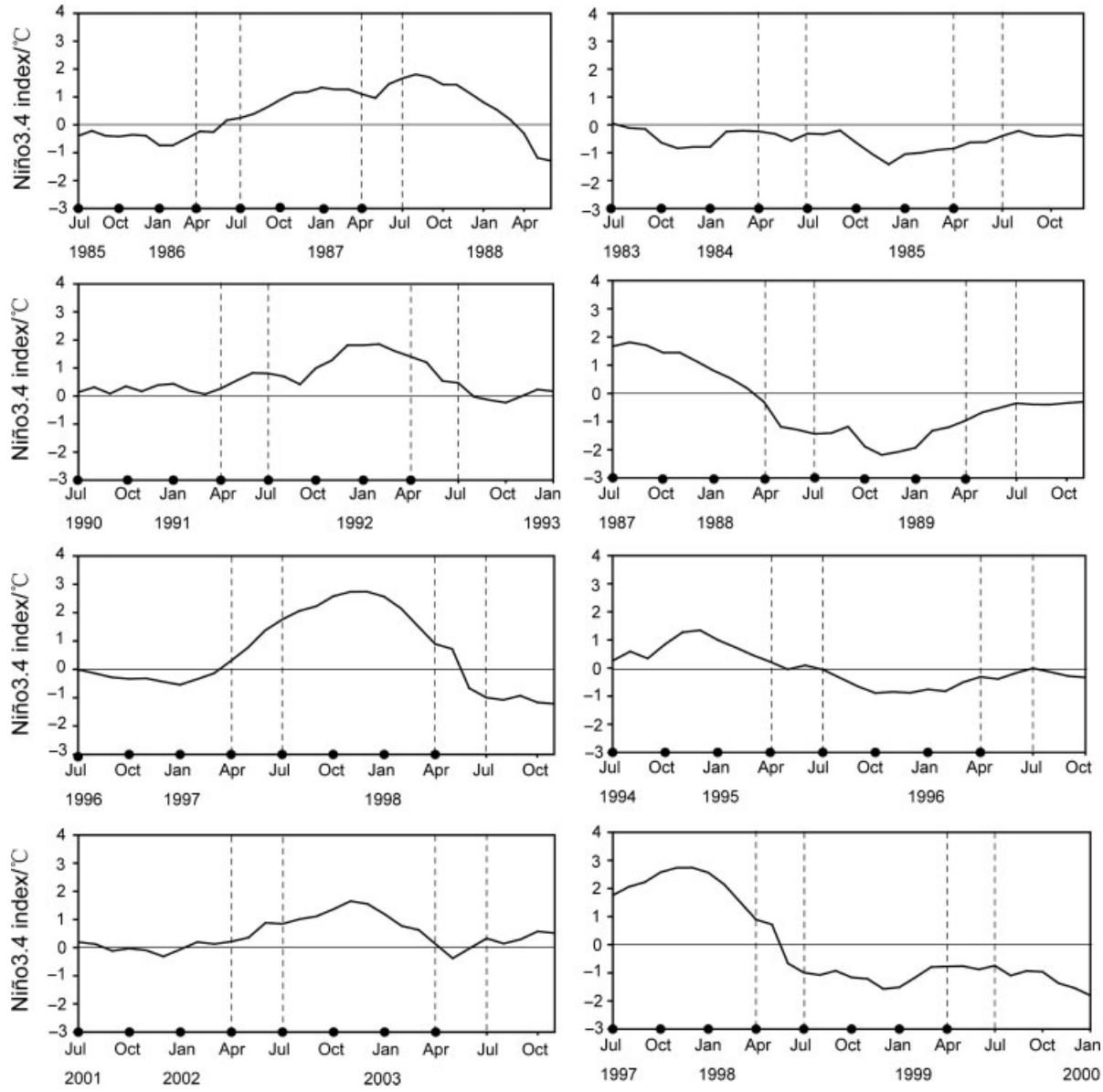


Figure 1. The observed Niño3.4 index of four El Niño events (left column) and La Niña events (right column) during 1982–2005. The start months of the predictions for these El Niño events are marked on the horizontal axis, where July (−1), October (−1), January (0) and April (0) are the start months of the growth-phase predictions and July (0), October (0), January (1) and April (1) are those of the decay-phase predictions. The dashed lines mark the spring (AMJ) in the growth-phase and decay-phase predictions.

to these predictions as growth-phase predictions. The El Nino/La Nina predictions with a start month of July (0), October (0), January (1) (i.e., January in Year (1)), and April (1) pass through the spring in the decay phase of El Nino/La Nina and are therefore referred to as decay-phase predictions hereafter.

## 3. The SPB phenomenon for ENSO predictions generated by the FGOALS-g model

Yan and Yu (2012) used the results of the ensemble forecast generated by the FGOALS-g model to investigate the forecasting skill by statistical analysis and found the SPB phenomenon of the predictions for SST in a probabilistic sense. Wei and Duan (2010) also used the SST predicted by the FGOALS-g model and preliminarily revealed the phenomenon of the SPB from the view of error growth. However, these papers cannot answer the questions posed in the introduction; i.e., do initial errors of realistic predictions that are similar to the CNOP errors and correspond to a significant SPB for El Nino events exist? In addition, what is the mechanism of the SPB for El Nino events in the imperfect model scenario? In this paper, we investigate these problems associated with SPB from the view of error growth.

A significant SPB here, as mentioned in the Introduction, refers to the phenomenon that ENSO forecasting has a large prediction error; in particular, a prominent error growth occurs during the spring when the prediction is made before the spring. In the following, we will address the SPB problem from two aspects: (1) the prediction

 

errors of the ENSO events and (2) their season-dependent evolution.

To study the season-dependent evolution of prediction errors, we divide a calendar year into four seasons starting with January to March (JFM), followed by April to June (AMJ), and so forth. The slope of the curve $\gamma(t) = ||T^{'}(t)||$ during different seasons was evaluated, where $T^{'}(t)$ represents the SSTA component of the evolutions of prediction errors for ENSO events. Then, the slopes, $\kappa = \frac{\partial \gamma(t)}{\partial t}$, of the curve $\gamma(t) = ||u(t)||$ for different seasons were estimated, where $u(t)$ represents the evolution of the prediction errors for El Nino events and the slope indicates the growth rates of the prediction errors for the different seasons. In particular, if we assume that the prediction error at the starting time of a season is $||u(t_1)||$ and at the end of the season is $||u(t_2)||$, the growth rate of the prediction error for the season can be roughly estimated by evaluating $\kappa \approx \frac{||u(t_2)|| - ||u(t_1)||}{t_2 - t_1}$. Because each season possesses a common time interval length, here we simply used the values of $||u(t_2)|| - ||u(t_1)||$ to indicate the tendency, $\kappa$, of the growth of the prediction errors for each season. A positive (negative) value of $\kappa$ implies an increase (decrease) in the error, and the larger the absolute value of $\kappa$, the faster the increase (decrease) in the error.

To apply the above strategy to study the season-dependent evolution of prediction errors, it was necessary to derive the SSTA from the SST forecasted by the FGOALS-g model. By calculating the mean values of the predicted SST, $\overline{T}^{p}$, at each month from 1982 to 2005, we obtained an annual cycle of model prediction and subtracted it from the predicted SST $T^{p}$, thus leading to a time series of 'predicted SSTA', $T_A^{p}$. In other words, we obtained the predicted SSTA by calculating $T_A^{p} = T^{p} - \overline{T}^{p}$. Using the observed SST $T^{O}$, we obtained the time series of the 'observed SSTA', $T_A^{O}$, with the realistic annual cycle $\overline{T}^{O}$, where the realistic annual cycle was obtained by taking the mean values of the observed SST during each month from 1982 to 2007. With the predicted SSTA $T_A^{p}$ and the observed one $T_A^{O}$, we obtained the prediction errors and then estimated their seasonal growth dependency.

It has been mentioned that, for an El Nino event, the predictions with a start month of July (−1), October (−1), January (0), and April (0) and a lead time of 12 months generally cross the boreal spring (April–May–June; AMJ) in the growth phase of the El Nino/La Nina event, while those with a start month of July (0), October (0), January (1) and April (1) often pass through the spring in the decay phase of the El Nino/La Nina event (except for the 1986/1987 El Nino and 1998/1999 La Nina events). To investigate the SPB phenomenon in these predictions, we estimated the seasonal growth rates (as measured by the slope $\kappa$) of the prediction errors. We demonstrate that the prediction errors in the growth-phase predictions for El Nino events exhibit significant season-dependent evolution, yielding a significant SPB, while those of the decay-phase predictions behave a less prominent season-dependent evolution even though they cause a larger uncertainty than those associated with the growth-phase predictions, thereby leading to a less prominent SPB. For La Nina events, we demonstrated that the predictions do not yield an obvious season-dependent evolution of prediction errors, not causing as prominent an SPB as that of the growth-phase predictions for El Nino events; however, they cause prediction uncertainties as significant as the El Nino predictions. This implies that the SPB aggressively limits the ENSO predictability, but the large uncertainties of the ENSO predictions may not necessarily be caused by the SPB. To illuminate these results, we describe the details of the season-dependent predictability of the four observed El Nino/La Nina events.

### 3.1. The predictions for El Niño events

As described above, predictions starting from July (−1), October (−1), January (0) and April (0) straddle the boreal spring (AMJ) in the growth phase of El Niño events and are called growth-phase predictions. Now, we describe the dynamical behaviour of the corresponding predictions errors. The evolution of the prediction errors, $\gamma(t)$, was obtained by removing the SSTA of the observed El Niño events from the predicted ones. In doing so, the error growth rate measured by the slope $\kappa$ could be evaluated. For each El Nino event, we present in Table I the mean values of the slopes $\kappa$ of the ten-member predictions with ten initial conditions and a start month of July (−1), which roughly measures the mean skill of the single forecasts. The prediction errors tended to have their largest growth rate in the AMJ season and exhibit significant season-dependent evolution. The AMJ season covers the spring and the beginning of the summer, which corresponds to the season in which most climate models yield the SPB for ENSO events. Therefore, when the predictions start in July (−1), the FGOALS-g model tends to yield a significant SPB for single forecasts of El Nino events. If we consider the results of ensemble forecasts for SST, the prediction errors for El Nino events are often reduced (Figure 2). As mentioned previously, a significant SPB involves a large prediction error and its obvious season-dependent evolution. Therefore, the reduction of the prediction error for ensemble forecasts leads us to think that the SPB phenomenon in the ensemble forecast is much weaker. It was therefore inferred that the SPB for

Table I. The mean of the error growth rates $k$ of single forecasts for El Niño with a start month of July (−1) (The bold characters indicate the seasons that have the greatest growth rate of prediction error).

| El Niño event | JAS | OND | JFM | AMJ |
|---|---|---|---|---|
| 1986/1987 | **14.2278** | 3.4130 | −8.6793 | −3.8856 |
| 1991/1992 | 3.3140 | 5.4718 | −6.1908 | **8.7512** |
| 1997/1998 | 1.2174 | 9.5280 | −3.2437 | **22.2288** |
| 2002/2003 | 2.3449 | 1.2414 | −1.8402 | **5.4251** |

 

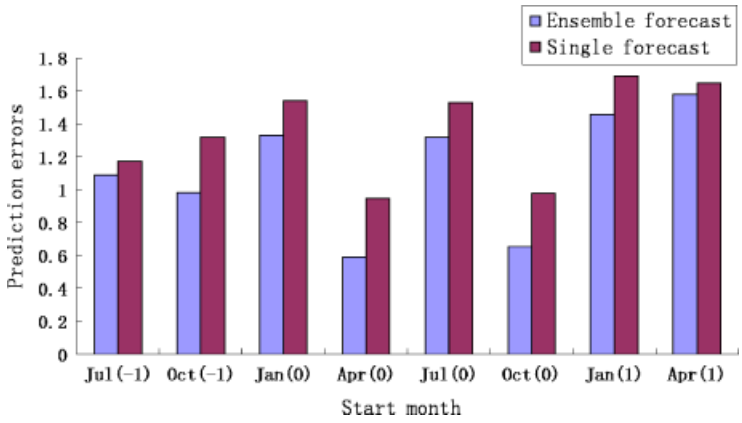


Figure 2. The prediction errors for single forecasts and ensemble forecasts. The former is obtained by taking the mean of the prediction errors of single forecasts for the four El Nino events; the latter is estimated by evaluating the mean of the prediction errors of the ensemble forecasts for the four El Nino events. The prediction errors for ensemble forecasts are often smaller than those for single forecasts, indicating that the ensemble forecast with different initial conditions to some extent reduces the prediction uncertainties for El Nino events.

Table II. The mean of the error growth rates $k$ of single forecasts for El Niño with a start month of October (−1). The bold characteristics are as in Table I.

| El Niño event | OND | JFM | AMJ | JAS |
|---|---|---|---|---|
| 1986/1987 | **16**.9614 | −1.8448 | −4.52499 | −0.3548 |
| 1991/1992 | 5.6249 | −7.2660 | **9**.9230 | 2.1911 |
| 1997/1998 | 8.7691 | 0.2048 | **16**.8357 | 5.1270 |
| 2002/2003 | −3.0759 | −2.8210 | **10**.6292 | 3.5060 |

Table III. The mean of the error growth rates $k$ of single forecasts for El Niño with a start month of January (0). The bold characteristics are as in Table I.

| El Niño event | JFM | AMJ | JAS | OND |
|---|---|---|---|---|
| 1986/1987 | **5.9027** | 5.4891 | −2.4275 | 6.6737 |
| 1991/1992 | 4.6695 | **15.1765** | −15.5694 | 11.1503 |
| 1997/1998 | 4.1496 | **16.5563** | −4.4389 | −1.7625 |
| 2002/2003 | 3.1286 | **22.2646** | −6.1001 | −0.3547 |

El Nino events may to some extent be related to initial uncertainties.

For the El Niño predictions starting from October (−1) and January (0), we also investigated the season-dependent evolution of the prediction errors for the four El Nino events (Tables II and III). The results illustrate that the prediction errors of these El Niño events tend to grow significantly during AMJ and yield a significant SPB; nevertheless, the ensemble forecast associated with multiple initial conditions reduce the SPB phenomenon to some extent (Figure 2). However, for the 1986/1987 El Nino event, the largest growth rates of the prediction errors were not always in the spring season for the predictions with different start months, so this event does not have a prominent SPB phenomenon.

Table IV. The mean of the error growth rates $k$ of single forecasts for El Niño with a start month of April (0). The bold characteristics are as in Table I.

| El Niño event | AMJ | JAS | OND | JFM |
|---|---|---|---|---|
| 1986/1987 | 0.3700 | **7.1942** | 1.5440 | −1.5109 |
| 1991/1992 | 5.4992 | **10.4252** | 5.2026 | −0.4553 |
| 1997/1998 | 2.9946 | −1.5612 | **6.5776** | −2.7369 |
| 2002/2003 | 2.2376 | **12.9754** | −6.0772 | −1.0929 |

Mu *et al.* (2007a) reported that the SPB is related to the annual cycle (also see Webster and Yang, 1992; Moore and Kleeman, 1996); that is, the seasonality of the predictability barrier originates from the annual cycle. The 1986/1987 El Nino event did not phase-lock to the annual cycle; that is, the peak of the 1986/1987 El Nino event did not occur at the end of the year, and the transition from the cold to the warm phase was not in the spring. This may be one of the reasons that the predictions of the 1986/1987 El Nino event do not yield a significant SPB.

We further explore the growth-phase predictions of El Niño with a start month of April (0) (Table IV). The month April (0) is the beginning of the AMJ season; therefore, the predictions initialized in April (0) start directly in the spring. In this situation, we demonstrate that the largest growth rate of the prediction errors for the four El Niño events does not occur in the AMJ season, implying that when the growth-phase predictions are made directly in the spring, the decrease in the skill seen during the spring (AMJ) is not nearly as significant. Furthermore, we find that the growth-phase predictions starting in April (0) yielded much smaller prediction uncertainties than those starting in other seasons (Figure 2); the growth-phase predictions are much more effective when they start in the spring than when they start in other seasons.

 

For the decay-phase predictions of the El Nino events, we also estimate the seasonal growth rate of the prediction errors. The results demonstrate that when the start month was July (0), the largest error growth rates of the El Niño events in 1991/1992, 1997/1998 and 2002/2003 are in the OND, AMJ and JAS seasons, respectively, whereas for the start month of October (0), the largest error growth rates of these three El Nino events are all in the OND season. For the start months of January (1) and April (1), the prediction errors have the largest growth rates in either the AMJ season or the OND season. However, for the 1986/1987 El Nino event, the decay phase did not include the spring season, and therefore, the decay-phase predictions did not involve the 1986/1987 El Nino. In any case, for the decay-phase predictions of the El Niño events, the largest error growth rates were not always in the spring season. The decay-phase predictions of the El Niño events present a nonobvious season-dependent evolution of prediction errors, thus causing a less prominent SPB. However, for either ensemble forecasts or single forecasts, the decay-phase predictions possessed a much larger prediction error and a poorer forecasting ability than the growth-phase predictions (Figure 3), although the growth-phase predictions exhibited a significant SPB phenomenon. Furthermore, the decay-phase predictions starting directly in the spring did not have a prediction error nearly as small as that of the growth-phase predictions. It is obvious that the forecast skill of El Nino predictions through spring depends on the phase of the El Nino events. Kirtman *et al*. (2002) reported that the ENSO predictions starting in the spring may have a much greater score than those starting in other seasons. Our results indicate that the greater score of the ENSO predictions with a spring start month may be reflected primarily in the growth-phase predictions for El Nino events.

When the predictions generated by the FGOALS-g model are made through the spring during the growth phase of El Nino events, the prediction errors tend to exhibit season-dependent growth and cause a large prediction error, thus yielding a significant SPB phenomenon. The ensemble forecast technique reduces the uncertainties of the forecasting through the spring and indicates that the SPB may be related to initial uncertainties. Although the decay-phase predictions of El Nino events have much larger uncertainties, they do not exhibit an obvious season-dependent evolution of prediction errors and do not exhibit a prominent SPB. The occurrence of the SPB depends on the phases of the El Nino events. Furthermore, the results indicate that a significant SPB implies a significant prediction uncertainty, but a large prediction uncertainty may not necessarily be caused by a significant SPB.

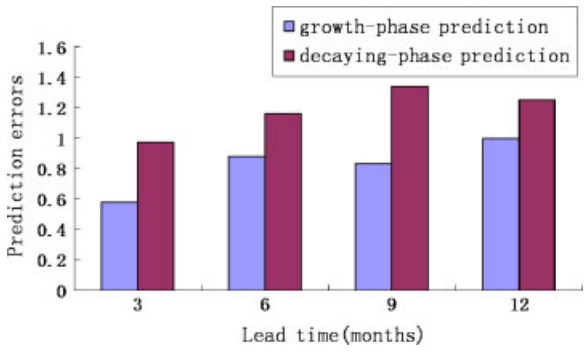


Figure 3. The prediction errors of single forecasts for the four El Nino events, which are for the growth-phase and the decay-phase predictions respectively. The prediction errors for the growth-phase predictions are often smaller than those for decay-phase predictions.

### 3.2. The predictions for La Nina events

From Section 3.1, we know that the El Niño growth-phase predictions tend to cause a prominent SPB, while the decay-phase predictions have a less significant SPB. In this section, we will investigate the SPB phenomenon for the La Niña predictions generated by the FGOALS-g model.

We studied the season-dependent evolutions of prediction errors for the four La Niña events from 1982 to 2005. The results demonstrate that neither the growth-phase predictions nor the decay-phase predictions exhibit a significant season-dependent evolution of prediction

Table V. The mean of the error growth rates $k$ of single forecasts for El Niño with a start month of July (−1). The bold characteristics are as in Table I.

| La Niña event | JAS | OND | JFM | AMJ |
|---|---|---|---|---|
| 1984/1985 | −1.7720 | −8.1956 | **21.1823** | −1.3639 |
| 1988/1989 | **19.6745** | −5.2589 | −5.8381 | 1.4092 |
| 1995/1996 | −1.2286 | **6.6341** | −8.2167 | −3.6610 |
| 1998/1999 | −1.6310 | 10.0125 | 11.1387 | **22.3826** |

Table VI. The mean of the error growth rates $k$ of single forecasts for El Niño with a start month of January (0). The bold characteristics are as in Table I.

| La Niña event | OND | JFM | AMJ | JAS |
|---|---|---|---|---|
| 1984/1985 | **20.6852** | −5.9568 | −15.9025 | −2.1503 |
| 1988/1989 | 0.8015 | **3.0969** | 0.1765 | 2.3241 |
| 1995/1996 | **11.9307** | 7.0700 | −14.2091 | −3.4893 |
| 1998/1999 | 0.3520 | 2.2753 | 8.9794 | **10.3351** |

Table VII. The mean of the error growth rates $k$ of single forecasts for El Niño with a start month of July (0). The bold characteristics are as in Table I.

| La Niña event | JAS | OND | JFM | AMJ |
|---|---|---|---|---|
| 1984/1985 | 3.8322 | **28.6102** | −7.5550 | −5.9142 |
| 1988/1989 | −1.7241 | **2.6647** | −5.7061 | 0.2726 |
| 1995/1996 | **4.8980** | −5.0450 | 0.8937 | 1.1813 |

Table VIII. The mean of the error growth rates $k$ of single forecasts for El Niño with a start month of January (1). The bold characteristics are as in Table I.

| La Niña event | JFM | AMJ | JAS | OND |
|---|---|---|---|---|
| 1984/1985 | −6.5301 | −0.6698 | **5.2977** | 5.0982 |
| 1988/1989 | −1.0639 | 2.7201 | **17.1540** | 5.5175 |
| 1995/1996 | −5.3403 | −1.8484 | **16.8388** | 8.1510 |

errors. In other words, the largest error growth rates of the predictions for the La Nina events generated by the FGOALS-g model are not in the same season, and in particular, they are not in the AMJ season. Tables V – VIII present the seasonal growth rates of the prediction errors for the growth-phase predictions with the start months of July (−1) and January (0) and for the decay-phase predictions with the start months of July (0) and January (1). For the decay-phase predictions through the spring, the 1998/1999 La Niña event is not displayed in Tables VII and VIII; the predictions starting in July (0), October (0), January (1) and April (1) did not pass through the spring in the decay phase of the 1998/1999 La Nina event, so the growth rates of the prediction errors are not included in the tables. The La Nina predictions did not present a prominent SPB, but they did cause a significant prediction uncertainty. This result further indicates that a large prediction error may not necessarily be caused by a significant SPB phenomenon.

The growth-phase predictions for the El Nino events were more effective than the decay-phase predictions. Does the same hold true for La Nina predictions? By comparing the prediction errors of the decay-phase predictions with those of the growth-phase predictions, we found that the growth-phase predictions for the La Nina events were much less effective than the decay-phase predictions (Figure 4). This characteristic of the La Nina predictions is not the same as that of the El Nino predictions.

In summary, a significant SPB does not occur for either the growth-phase or the decay-phase predictions of La Niña events, while a prominent SPB does occur in the growth-phase predictions of El Nino events. Despite this, the growth-phase predictions for El Nino events possess a greater score than the decay-phase predictions, but the growth-phase predictions for La Nina events reveal a lower forecast skill than the decay-phase predictions. These results indicate that the forecast skill of ENSO predictions through the spring is closely related to ENSO events themselves and that the El Nino predictions may have different behaviour than the La Nina predictions. Furthermore, the significant SPB of the El Nino growth-phase predictions causes large prediction errors, but the large errors for the El Nino decaying-phase predictions and the La Nina growth- and decaying-phase predictions may not be necessarily caused by a significant SPB phenomenon. In any case, the SPB is still a very important factor that aggressively limits the ENSO predictability. It is very necessary to reveal the SPB phenomenon and clarify the possible mechanism of the SPB, which will benefit the improvement of the ENSO forecasting skill.

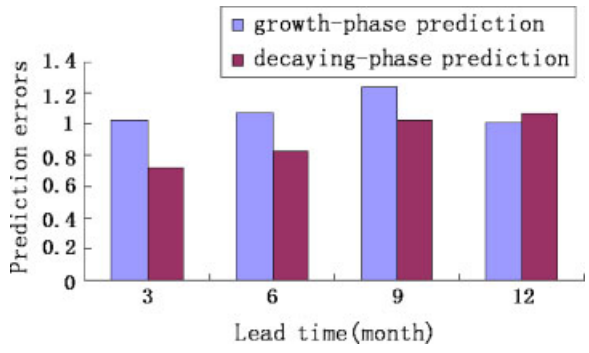


Figure 4. The prediction errors of single forecasts for the four La Nina events, which are for the growth-phase and the decay-phase predictions respectively. The prediction errors for the growth-phase predictions are often larger than those for decay-phase predictions.

## 4. Possible mechanism of SPB for El Nino events

In Section 3, we demonstrated that the growth-phase predictions of El Nino events tend to yield a significant SPB. Duan *et al*. (2009) and Yu *et al*. (2009) conducted perfect model predictability experiments with the Zebiak–Cane model (Zebiak and Cane, 1987) and revealed that two types of initial errors exist that are most likely to cause a significant SPB for El Nino events. One type of initial error has an SSTA pattern with negative anomalies in the equatorial central-western Pacific and positive anomalies in the equatorial eastern Pacific; the other type of initial error has patterns nearly opposite to those of the former type. To facilitate the discussion, we refer to the former error pattern as a Type A error and the latter as a Type B error. These results were derived from perfect model predictability experiments with the Zebiak–Cane model (Zebiak and Cane, 1987); however, in more realistic predictions (e.g., the hind-cast experiments generated by the FGOALS-g model), not only initial errors but also model errors exist. That is to say, the hindcast experiments are often within the framework of imperfect model predictability experiments. Fundamental questions must be addressed, including the following: (1) in realistic predictions, do the Type A and B initial errors that correspond to a significant SPB for El Nino events exist? (2) What is the mechanism of the SPB for El Nino events in an imperfect model scenario?

### 4.1. Do the Type A and B errors exist in the ENSO predictions generated by the FGOALS-g model?

We investigated the spatial patterns of the initial SST errors that correspond to a significant SPB for realistic ENSO predictions generated by the FGOALS-g model. For each El Nino event, there were eight start months in the realistic predictions generated by the FGOALS-g model (see Section 2). At each start month, there were ten single forecasts with ten different initial monthly

 

SSTs (see Section 2). There was a total of 320 predictions for four realistic El Nino events. Statistically, 136 predictions exist that yield a significant SPB phenomenon with the greatest error growth rate occurring in the spring season. Furthermore, most of these predictions were growth-phase predictions, which coincide with the results of Section 3; that is, the growth-phase predictions potentially yielded a significant SPB for the El Nino events. For the SST component of the initial conditions of the 136 predictions, we obtained 136 initial error patterns by comparing the observed SSTA with the initial SSTA field of predictions. For these 136 initial SSTA error patterns, we performed an Empirical Orthogonal Function (EOF) analysis to identify the dominant mode of the initial SSTA errors. This mode is the dominant mode of the initial SSTA errors that correspond to a significant SPB for El Nino events. Figure 5 plots the spatial pattern of the leading EOF mode and the corresponding time series. The leading EOF mode accounted for 51% of the total variance over the region (170°E–85°W, 10°N–10°S), which approximately covers the Nino 3 and 4 regions. The leading EOF mode clearly demonstrated an SSTA pattern with negative anomalies in the equatorial central-western Pacific and positive anomalies in the equatorial eastern Pacific. From the time series of this leading EOF mode, we can see that the first EOF mode exhibited not only a positive phase but also a negative phase, which indicates that the dominant mode of the initial SSTA errors could be either the pattern illustrated in Figure 5 (Pattern A; corresponding to the positive phase of the time coefficient series) or its opposite pattern (Pattern B; corresponding to the negative phase of the time coefficient series). Furthermore, both Patterns A and B bear great resemblance to the Types A and B errors mentioned above, respectively. Therefore, we demonstrated that in realistic ENSO predictions generated by the FGOALS-g model, initial SSTA errors exist that are similar to those of the Type A and B errors reported by Yu *et al.* (2009) and Duan *et al.* (2009), and they also correspond to a significant SPB for El Nino events.

### 4.2. Behaviour of error growth related to the SPB for El Nino events

From Figure 5, we noticed that the time coefficient series of the first EOF mode displayed its positive phase in most of the 136 El Nino predictions. This implies that for the El Nino predictions, most contained the initial SSTA errors with the dominant mode illustrated in Figure 5, and the rest of the 136 predictions had the initial SSTA errors with the major mode opposite that in Figure 5. In addition, Duan *et al.* (2009) and Yu *et al.* (2009) demonstrated that the Type A and B errors physically favour anomalous westerlies and easterlies along the equator and are most likely to evolve into El Nino- and La Nina-like events, respectively, in the Zebiak–Cane model (Zebiak-Cane, 1987). One can therefore ask whether, in the ENSO predictions generated by the FGOALS-g model, the dominant modes of the initial SSTA errors (i.e., the Pattern A and B modes, which are similar to the Type A and B errors) correspond to El Nino- and La Nina-like events. The answer to this question will help identify the behaviour of the error growth related to the SPB for El Nino events.

To address this question, we explored the time-dependent evolution of the prediction errors corresponding to the 136 initial errors. The 136 time-dependent series of prediction errors were 12 months in length, corresponding to the leading time 12 months of predictions. We divided each 12-month time series into four consecutive quarters; i.e., the first through the third month

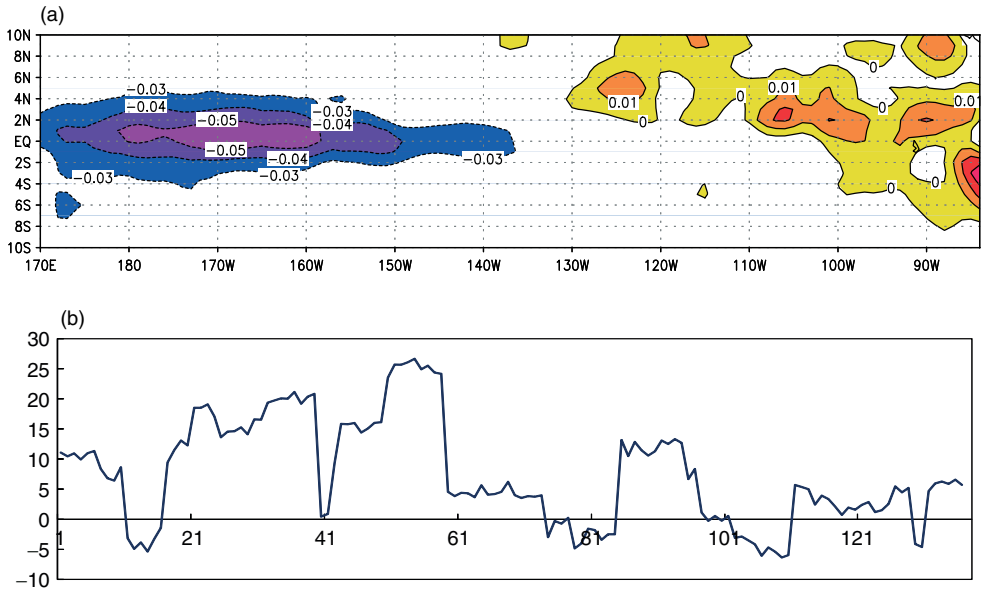


Figure 5. (a) The leading EOF mode of the 136 initial errors that corresponded to a significant SPB for the El Nino events and (b) the corresponding time series. The numbers located on the horizontal axis in (b) represents the 136 predictions for the El Nino events. Each number corresponds to one prediction.

 

(season-1), the fourth through the sixth month (season-2), and so forth. By applying the season-reliant EOF analysis (S-EOF) method (Wang and An, 2005), we detected the major mode of the season-dependent evolutions of the prediction errors over the Nino 3 and 4 regions. The S-EOF method can be used to search for the seasonally evolving patterns from year to year. The spatial pattern obtained for each S-EOF mode describes the evolving seasonal anomalies in a given year. These patterns share the same yearly value in the corresponding principal component (PC; for details, please see Wang and An, 2005). In this study, we connected the 136 time-dependent series and regarded them as a time series of year-to-year variations. The prediction errors in the four sequential seasons were then treated as an integral block to construct a covariance matrix. After the EOF decomposition was performed, the yearly block was divided into four sequential seasonal prediction errors so that a PC was derived for each eigenvector that contained a set of seasonally evolving patterns of the prediction errors from season-1 to season-4.

Figure 6 illustrates the first S-EOF mode and the corresponding time series, which accounts for 64% of the total variance. This seasonally evolving mode of SSTA errors corresponds to the positive phase of the time series and is the seasonally evolving major mode of the prediction errors that causes a significant SPB for the El Nino events. For convenience, we denote this mode as Evolution A mode. This seasonally evolving dominant mode of the prediction errors clearly seems to be an El Nino evolving mode; however, the time coefficient series of the first S-EOF mode also displays a negative phase in some predictions (Figure 6). This result indicates that in these predictions, the pattern of the seasonally evolving major mode of prediction errors is opposite that illustrated in Figure 6; that is, in these predictions, the prediction errors, which cause a significant SPB for El Nino events, display a La Nina-like evolving major mode and have dynamical behaviour opposite the El Nino events. We refer to this mode as the Evolution B mode. It is clear that the prediction errors that yield a significant SPB tend to have seasonally evolving major patterns as El Nino or a La Nina evolving modes. This implies that the error growth associated with the SPB for El Nino events possesses the same mechanism as the ENSO events themselves.

We have demonstrated that in realistic predictions generated by the FGOALS-g model, the initial SSTA errors that correspond to a significant SPB have the dominant modes of Patterns A and B, which are very similar to the Type A and B errors reported by Yu *et al*. (2009) and Duan *et al*. (2009). Furthermore, the prediction errors demonstrate seasonally evolving major modes of the Evolution A and B modes, like the El Nino and La Nina evolving modes, respectively. From Figure 5, it is apparent that the Pattern A mode of initial errors arises in most of the 136 El Nino predictions, while the Pattern B mode, opposite from Pattern A, appears in the rest of the 136 predictions. By comparing the time coefficient series in Figures 5 and 6, we find that the seasonally evolving major modes of prediction errors, Evolution A (B), arose in almost all of the predictions corresponding to Pattern B (A) of the initial errors. This means that the dominant mode of the initial SSTA errors, Pattern A (B), approximately corresponded to the seasonally evolving major mode of prediction errors, Evolution B (A). However, as mentioned previously, the Type A (B) errors in the Zebiak–Cane model potentially physically activate an anomalous westerly (easterly) and favor an El Nino (a La Nina) evolving mode, while in the ENSO predictions generated by the FGOALS-g model, the initial errors of the dominant mode of Pattern A (Pattern B) correspond to the seasonally evolving major mode, the Evolution B (A) mode, which corresponds to a La Nina (an El Nino) evolving mode. That is, Patterns A and B should have physically developed into the Evolution A and B major modes, but they tended to have an opposite trend in the predictions generated by the imperfect FGOALS-g model. Therefore, we naturally ask whether it is model error or initial errors of other variables that causes this difference between Type A (B) and Pattern A (B). If it is due to model errors, we will have to demonstrate that the model errors will also have a significant season-dependent evolution and lead to a prominent SPB for the El Nino events. Of course, this is only an assumption, which will be examined in future papers by comparing the results of a perfect model assumption with those of an imperfect model scenario.

At all events, we have demonstrated that the prediction errors that yield a significant SPB tend to have seasonally evolving major patterns of an El Nino or a La Nina evolving mode. The prediction errors that have similar dynamic behaviour to El Nino and La Nina events may easily cause a significant SPB for El Nino events. The El Nino and La Nina events are now understood to develop as a result of Bjerknes' (1969) positive feedback; meanwhile, they usually exhibit the fastest growth during the spring (Moore and Kleeman, 1996), as the spring maintains the strongest ocean-atmospheric instability of the climatological annual cycle (Wang *et al*., 1996). The prediction errors that have similar dynamical behaviour to El Nino and La Nina events may be the most likely to cause a significant SPB for El Nino events. Therefore, no matter what the initial errors are like, the prediction errors caused by the initial errors and the model errors will be more likely to cause a significant SPB for El Nino events if and only if they exhibit an El Nino or a La Nina evolving mode.

## 5. Summary and discussion

The SPB problem in ENSO predictions was explored by analysing the predictions generated by the FGOALS-g model. The results demonstrate that the SPB phenomenon exists for El Nino events in the ENSO predictions generated by the FGOALS-g model. In particular, the predictions through the spring season during the growth

 

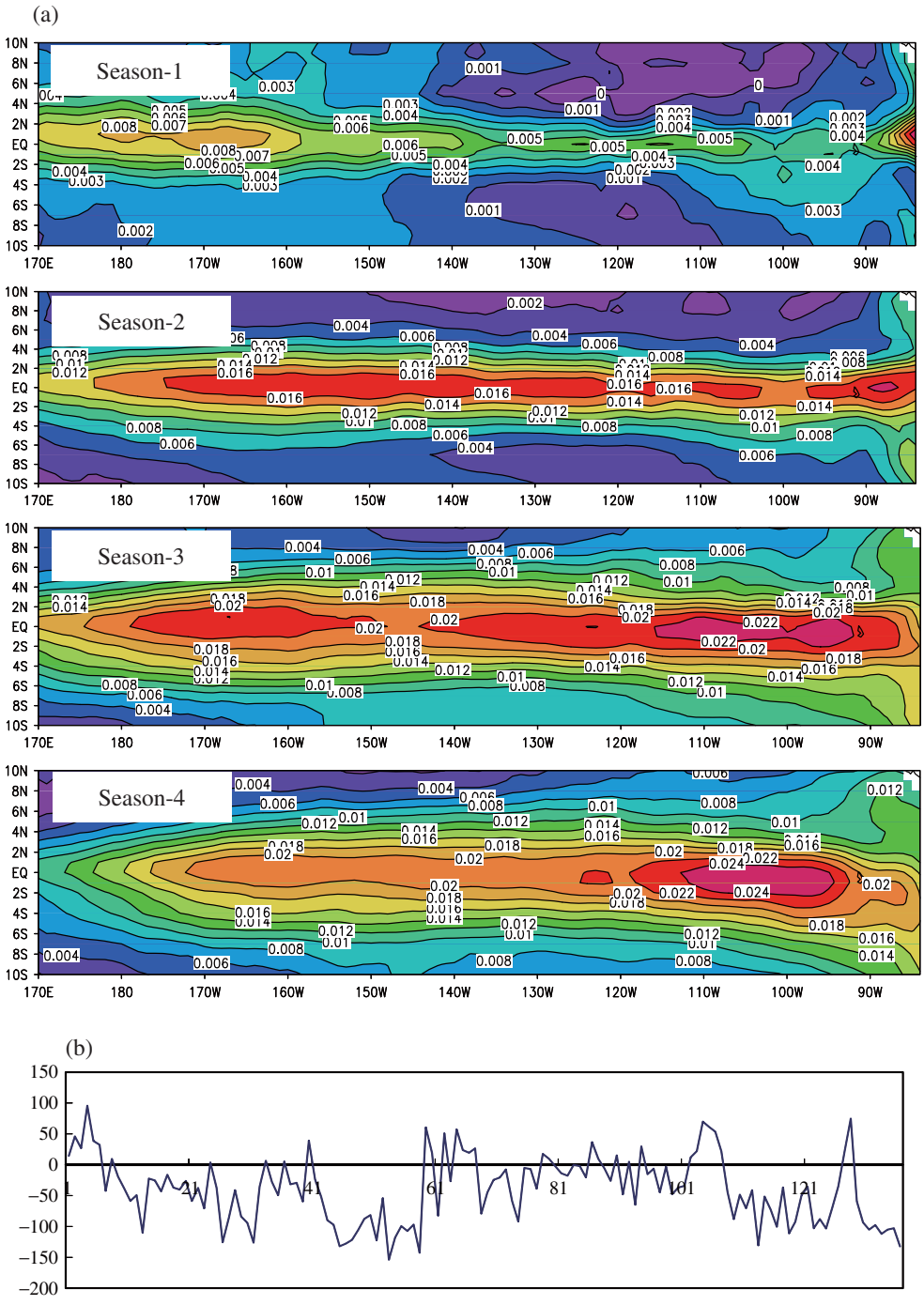


Figure 6. (a) The seasonally evolving major mode of prediction errors that caused a significant SPB for the El Nino events and its corresponding time series. The horizontal axis in (b) is as in Figure 5.

phase of the El Nino events demonstrated a much more significant SPB than the other predictions did. The ensemble forecast with multiple initial conditions alleviated the SPB phenomenon due to the reduction of prediction errors, which indicates that the SPB is to some extent related to initial errors. The results also indicate that the predictions that began directly in the spring season during the growth phase of the El Nino events may have much smaller prediction errors than the predictions that began in other seasons. Therefore, the results reported by Kirtman *et al*. (2002), that the predictions with a start month in the spring are relatively more effective than those with a start month in other seasons, may be primarily reflected in the predictions with a start month in the spring during the growth phase of El Nino events.

We demonstrated that the initial errors that correspond to a significant SPB for El Nino predictions generated by the FGOALS-g model had statistically major modes corresponding to Patterns A and B, similar to the Type A and B errors reported by Duan *et al*. (2009) and Yu *et al*. (2009). Meanwhile, we demonstrated that the prediction

 

errors that caused a significant SPB exhibited the same seasonally evolving major modes as the El Nino or La Nina evolving modes, which indicates that a significant SPB may result from the prediction errors having similar dynamic behaviour to El Nino and La Nina events; that is, from the Bjerknes' positive feedback mechanism. Yu *et al*. (2009) and Duan *et al*. (2009) demonstrated that the Type A (B) errors of the SSTA pattern with negative (positive) anomalies in the equatorial central-western Pacific and positive (negative) anomalies in the equatorial eastern Pacific have dynamic behaviour similar to El Nino (La Nina) events. However, Patterns A and B, similar to Types A and B in the El Nino predictions generated by the FGOALS-g model, correspond to La Nina and El Nino evolving modes, respectively. This difference between Yu *et al*. (2009) (also see Duan *et al*., 2009) and the present study will be investigated in future papers by performing many experiments within the framework of a perfect model and an imperfect mode. In fact, regardless of the types of errors that play an important role in yielding prediction uncertainties related to SPB, the prediction errors induced by them that exhibit the seasonally evolving major modes as El Nino or La Nina evolving modes will be the most likely to cause a significant SPB, although these two major evolving modes did not physically result from Patterns A and B.

Kirtman *et al*. (2002) compared the status of ENSO forecasts generated by a group of international climate models. From Figure 4 in Kirtman *et al*. (2002), it can easily be seen that the predictions generated by the University of Oxford (UOX) coupled model (Balmaseda *et al*., 1994) and the Linear Inverse Modelling (LIM) prediction system (Penland and Magorian, 1993) with observational data as the initial conditions exhibited a significant SPB for ENSO events. This indicates that the prediction errors generated by these two models were only caused by the model errors, but they also caused a significant SPB for ENSO events. Furthermore, Zheng and Zhu (2010) demonstrated that the SPB can be reduced by using the random forcing to offset the model errors. We have demonstrated that the Pattern A and B error modes correspond to different tendencies of prediction error evolutions from those of the Type A and B errors. Is this difference caused by the model errors as in the UOX and LIM models? This is a very challenging question that must be explored by conducting many experiments running the FGOALS-g model in the scenarios of a perfect model and an imperfect model.

In addition, this paper adopted the definition of SPB as the phenomenon of ENSO forecasting having a large prediction error; in particular, a prominent error growth occurs during the spring when the prediction is made before and throughout the spring. Some studies also used the decline of the forecasting skill, such as the anomaly correlation, to describe the SPB. Zheng and Zhu (2010) indicated that the rapid spring decline of the anomaly correlation skill for El Nino predictions accompanies the rapid growth of the prediction errors in the spring. This implies that the SPB described by the anomaly correlation skill of the predictions is in accordance with that described by the prediction errors. Nevertheless, the SPB described in the present study can identify the predictions that display a less prominent SPB with negligible prediction errors but obvious season-dependent evolution of prediction errors or less significant season-dependent evolution of prediction errors but a large prediction error.

The SPB for ENSO is an unresolved problem, though it has attracted the attention of many scientists. This paper reveals the SPB phenomenon of the predictions generated by the FGOALS-g model and finds the CNOP-like errors associated with SPB, finally demonstrating the mechanism of the SPB in the imperfect model scenario. These results extend those of Yu *et al*. (2009) and Duan *et al*. (2009) and emphasize that the CNOP-like errors related to SPB and the SPB's mechanism demonstrated by Duan *et al*. (2009) and Yu *et al*. (2009) are still valid in realistic ENSO predictions generated by the FGOALS-g model. This outcome encourages us to filter the CNOP-like errors by appropriate approaches and perform ensemble forecasting to reduce the effect of SPB on prediction uncertainties. The model error is also an important source of prediction errors. As mentioned previously, its effect on SPB for El Nino events may exist, which should therefore be explored in depth. Furthermore, model errors come from different sources, such as model parameter errors, the uncertainties of some physical processes, the errors in external forces, and the uncertainties of the computation scheme, among others. It is unknown which type of model error plays the dominant role in producing prediction uncertainties or which kind of model error should be prioritized for improvement. All of these should be investigated in future in-depth studies. The results from this study are expected to provide useful information for ensemble forecasting with multiple physical processes, external forcing, and more.

## Acknowledgements

This work was jointly sponsored by the National Basic Research Program of China (Nos. 2012CB955202, 2010CB950402), Knowledge Innovation Program of the Chinese Academy of Sciences (No. KZCX2-YW-QN203), the National Natural Science Foundation of China (No.41176013).

## References

Balmaseda MA, Anderson DLT, Davey MK. 1994. ENSO prediction using a dynamical ocean model coupled to a statistical atmospheres. *Tellus* **46A**: 497–511.

Bjerknes J. 1969. Atmospheric teleconnections from the equatorial Pacific. *Monthly Weather Review* **97**: 163–172.

Bonan GB, Oleson KW, Vertenstein M, Leviss S, Zeng XB, Dai YJ, Dickinson RE, Yang ZL. 2002. The land surface climatology of the community land model coupled to the NCAR community climate model. *Journal of Climate* **15**: 3123–3149.

Chen D, Zebiak SE, Busalacchi AJ, Cane MA. 1995. An improved procedure for El Niño forecasting : Implications for predictability. *Science* **269**: 1699–1702.

Chen D, Cane MA, Kaplan A, Zebiak SE, Huang DJ. 2004. Predictability of El Niño over the past 148 years. *Nature* **428**: 733–736.

 

Duan WS, Mu M. 2006. Investigating decadal variability of El Niño–Southern Oscillation asymmetry by conditional nonlinear optimal perturbation. *Journal of Geophysical Research* **111**: C07015, DOI:10.1029/2005JC003458.

Duan WS, Mu M, Wang B. 2004. Conditional nonlinear optimal perturbation as the optimal precursors for ENSO events. *Journal of Geophysical Research* **109**: D23105.

Duan WS, Xu H, Mu M. 2008. Decisive role of nonlinear temperature advection in El Ni˜ no and La Ni˜ na amplitude asymmetry. *Journal of Geophysical Research* **113**: C01014 DOI:10.1029/2006JC003974.

Duan WS, Liu XC, Zhu KY, Mu M. 2009. Exploring the characteristic of initial errors that cause a significant "spring predictability barrier" for El Nino events. *Journal of Geophysical Research* **114**: C04022, DOI: 10.1029/2008JC004925.

Jin FF. 1997a. An equatorial ocean recharge paradigm for ENSO. Part I: Conceptual model. *Journal of Atmospheric Sciences* **54**: 811–829.

Jin FF. 1997b. An equatorial ocean recharge paradigm for ENSO. Part II. A stripped-down coupled model. *Journal of Atmospheric Sciences* **54**: 830–847.

Jin EK, Kinter III JL, Wang B, Park CK, Kang IS, Kirtman BP, Kug JS, Kumar A, Luo JJ, Schemm J, Shukla J, Yamagata T. 2008. Current status of ENSO prediction skill in coupled ocean-atmosphere models. *Climate Dynamics* **31**: 647–664.

Kauffman BG, Large WG. 2002. The CCSM coupler version 5.01: combined user's guide, source code reference and scientific description, National Center for Atmospheric Research, Boulder, Colorado, USA, 46pp.

Kleeman R. 1993. On the dependence of hindcast skill on ocean thermodynamics in a coupled ocean-atmosphere model. *Journal of Climate* **6**: 2012–2033.

Kleeman R, Moore AM, Smith NR. 1995. Assimilation of sub-surface thermal data into an intermediate tropical coupled ocean-atmosphere model. *Monthly Weather Review* **123**: 3103–3113.

Kirtman, BP, Shukla J, Balmaseda M, Graham N, Penland C, Xue Y, Zebiak S. 2002. Current status of ENSO forecast skill: A report to the Climate Variability and Predictability (CLIVAR) Numerical Experimentation Group (NEG), CLIVAR Working Group on Seasonal to Interannual Prediction, Clim. Variability and Predictability, Southampton Oceanogr. Cent., Southampton, UK.

Kiehl JT, Hack J, Bonan G, Boville BA, Briegleb BP, Williamson DL, Rasch PJ. 1996. Description of the NCAR Community Climate Model (CCM3), technical report NCAR/TN-420+STR, National Center for Atmospheric Research, Boulder, Colorado, USA, 152pp.

Lau KM, Yang S. 1996. The Asian monsoon and predictability of the tropical ocean-atmosphere system. *Quarterly Journal of Royal Meteorological Society* **122**: 945–957.

Liu HL, Zhang XH, Li W, Yu YQ, Yu RC. 2004. An eddy-permitting oceanic general circulation model and its preliminary evaluation. *Advances in Atmospheric Science* **21**: 675–690.

Li L, Wang B, Wang YQ, Wang H. 2007. Improvements in climate simulation with modifications to the Tiedtke convective parameterization in the grid-point atmospheric model of IAP LASG (GAMIL). *Advances in Atmospheric Sciences* **24**: 323–335.

Luo JJ, Masson S, Behera S, Yamagata T. 2008. Extended ENSO predictions using a fully coupled ocean-atmosphere model. *Journal of Climate* **21**: 84–93.

McCreary JP, Anderson DLT. 1991. An overview of coupled ocean-atmosphere models of El Nino and Southern oscillation. *Journal of Geophysical Research* **96**: 3125–3150.

McPhaden MJ. 2003. Tropical Pacific ocean heat content variations and ENSO persistence barriers. *Geophysical Research Letters* **30**: 1480, DOI: 10.1029/2003GL016872.

Moore AM, Kleeman R. 1996. The dynamics of error growth and predictability in a coupled model of ENSO. *Quarterly Journal of Royal Meteorological Society* **122**: 1405–1446.

Mu M, Zhang Z. 2006. Conditional nonlinear optimal perturbations of a two-dimensional quasigeostrophic model. *Journal of Atmospheric Sciences* **63**: 1587–1604.

Mu M, Duan WS, Wang B. 2003. Conditional nonlinear optimal perturbation and its applications. *Nonlinear Processes in Geophysics* **10**: 493–501.

Mu M, Duan WS, Wang B. 2007a. Season-dependent dynamics of nonlinear optimal error growth and El Niño-Southern Oscillation predictability in a theoretical model. *Journal of Geophysical Research* **112**: D10113, DOI: 10.1029/2005JD006981.

Mu M, Xu H, Duan WS. 2007b. A kind of initial errors related to "spring predictability barrier" for El Niño events in Zebiak-Cane model. *Geophysical Research Letters* **34**: L03709, DOI: 10.1029/2006GL-27412.

Palmer TN, Doblas-Reyes FJ, Hagedorn R, Alessandri A, Gualdi S, Andersen U, Feddersen H, Cantelaube P, Terres J-M, Davey M, Graham R, Délécluse P, Lazar A, Déqué M, Guérémy J-F, Díez E, Orfila B, Hoshen M, Morse AP, Keenlyside N, Latif M, Maisonnave E, Rogel P, Marletto V, Thomson MC. 2004. Development of a European multimodel ensemble system for seasonal-to-interannual prediction (DEMETER). *Bulletin of the American Meteorological Society* **85**: 853–872.

Penland C, Magorian T. 1993. Prediction of Niño-3 sea surface temperatures using linear inverse modeling. *Journal of Climate* **6**: 1067–1076.

Reynolds RW, Rayner NA, Smith TM, *et al*. 2002. An improved in situ and satellite SST analysis for climate. *Journal of Climate* **15**: 1609–1625.

Samelson RG, Tziperman E. 2001. Instability of the chaotic ENSO: the growth-phase predictability barrier. *Journal of Atmospheric Sciences* **58**: 3613–3625.

Saha S, Nadiga S, Thiaw C, Wang J, Wang W, Zhang Q., van den Dool HM, Pan H-L, Moorthi S, Behringer D, Stokes D, Pena M, Lord S, White G, Ebisuzaki W, Peng P, Xie P. 2006. The NCEP Climate Forecast System. *Journal of Climate* **19**: 3483–3517.

van Oldenborgh GJ, Balmaseda MA, Ferranti L, Stockdale TN, Anderson DLT. 2005. Evaluation of atmospheric fields from the ECMWF seasonal forecasts over a 15-year period. *Journal of Climate* **18**: 3250–3269.

Wang B, An S-II. 2005. A method for detecting season-dependent modes of climate variability: S-EOF analysis. *Geophysical Research Letters* **32**: L15710, DOI: 10.1029/2005GL022709.

Wang B, Fang Z. 1996. Chaotic oscillation of tropic climate: a dynamic system theory for ENSO. *Journal of Atmospheric Sciences* **53**: 2786–2802.

Wang C, Picaut J. 2004. Understanding ENSO physics – a review. Earth climate: the ocean-atmosphere interaction. *Geophysical Monograph Series American Geophysical Union* **147**: 21–48.

Wang B, Fang Z. 1996. Chaotic oscillation of tropical climate: A dynamic system theory for ENSO, *Journal of the Atmospheric Sciences* **53**: 2786–2802.

Wang B, Barcilon A., Fang Z. 1999. Stochastic dynamics of El Niño-Southern Oscillation. *Journal of Atmospheric Sciences* **56**: 5–23.

Wang B, Wan H, Ji ZZ, Zhang X, Yu RC, Yu YQ, Liu HT. 2004. Design of a new dynamical core for global atmospheric models based on some efficient numerical methods. *Science in China* **47**: 4–21.

Weatherly JW, Briegleb BP, Large WG. 1998. Sea ice and polar climate in the NCAR CSM. *Journal of Climate* **11**: 1472–1486.

Webster PJ. 1995. The annual cycle and the predictability of the tropical coupled ocean-atmosphere system. *Meteorology and Atmospheric Physics* **56**: 33–55.

Webster PJ, Yang S. 1992. Monsoon and ENSO: Selectively interactive systems. *Quarterly Journal of Royal Meteorological Society* **118**: 877–926.

Wei C, Duan WS. 2010. The spring predictability barrier phenomenon of ENSO predictions generated with the FGOALS-g model. *Atmospheric and Oceanic Science Letters* **3**: 87–92.

Xue Y, Cane MA, Zebiak SE, Blumenthal MB. 1994. On the prediction of ENSO: a study with a low order Markov model. *Tellus* **46A**: 512–528.

Yan L, Yu YQ. 2012. The spring prediction barrier in ENSO hindcast experiments of FGOALS-g model. *Chinese Journal of Oceanology and Limnology* DOI: 10.1007/s00343-012-1271-z.

Yu YQ, Yu RC, Zhang XH, Liu HL. 2002. A flexible coupled ocean-atmosphere general circulation model. *Advances in Atmospheric Sciences* **19**: 169–190.

Yu YQ, Zhang XH, Guo YF. 2004. Global coupled ocean-atmosphere general circulation models in LASG/IAP. *Advances in Atmospheric Sciences* **21**: 444–455.

Yu YS, Duan WS, Xu H, Mu M. 2009. Dynamics of nonlinear error growth and season-dependent predictability of El Nino events in the Zebiak–Cane model. *Quarterly Journal of Royal Meteorological Society*. **25**(4): 1263–1277.

Zebiak SE, Cane A. 1987. A model El Niño-Southern Oscillation. *Monthly Weather Review* **115**: 2262–2278.

Zheng F, Zhu J. 2010. Spring predictability barrier of ENSO events from the perspective of an ensemble prediction system. *Global and Planetary Change* **72**: 108–117.

 